Mapping Historical Tsetse Fly distributions in Southern Africa

Purchase Order RAF5051 – 88126E

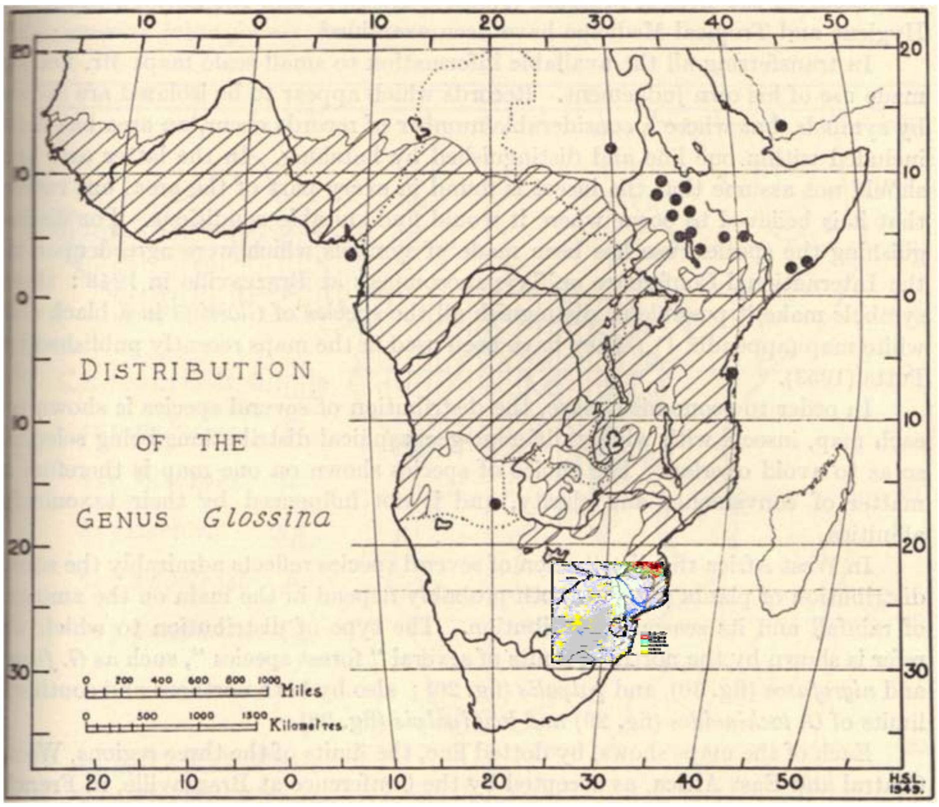

William Wint
Environmental Research Group Oxford
P.O. Box 346,
OXFORD, OX1 3QE
Tel: +44 1865 271257 / +44 1584819574
http://ergodd.zoo.ox.ac.uk
Email: william.wint@zoo.ox.ac.uk

August 2008

Cover illustration: An historical distribution of the Genus *Glossina* in Africa, prepared by H.S Leeson in 1949, published in Buxton, P. (1955) The Natural History of Tsetse Flies: An Account of the Biology of the Genus Glossina (Diptera). London, UK: H.K. Lewis & Co. Overlay for southern Africa is current distribution of *G. morsitans*, Figure 6

Table of Contents

List of Figures and Maps

List of Tables

Acknowledgements

Thanks are due to Rob Bagnall, Karin Kappmeier, Marc Vreysen and Udo Feldmann for advice and assistance with this work; and to Professor David Rogers and the Spatial Epidemiology and Ecology Group for processing the satellite imagery.

1) Introduction and Background

Figure 1: Transfrontier Park

The distribution of *G. morsitans* has changed markedly from its historical distributions of the early 20th Century, due both to active clearance programmes, and to displacement by expanding human activity. Plans to create a Greater Limpopo Trans Frontier Park (GL-TFP), which includes the Kruger National Park, Gonarezhou (Zimbabwe) and Limpopo National Park (Mozambique). involve the creation of a number of wildlife corridors to allow the free movement of animals from one section of the new park to another. Some epidemiologists are concerned that the movement of wild animals through these corridors might allow the spread of trypanosomiasis and its insect vector *Glossina* to areas where it has not been present for many years.

It will therefore be necessary to prepare maps of the potential distribution of the tsetse fly in order to assess the risk trypanosomiasis spreading. The methods need to do this have been developed by IAEA commissioned consultancies, and have been used to produce a series of maps for a number tsetse fly species in several parts of Africa (*http://ergodd.zoo.ox.ac.uk/tseweb/iaea/1kmtse.htm*). These have been widely used to assess disease risk and target tsetse control priorities

Figure 2: Required map coverage

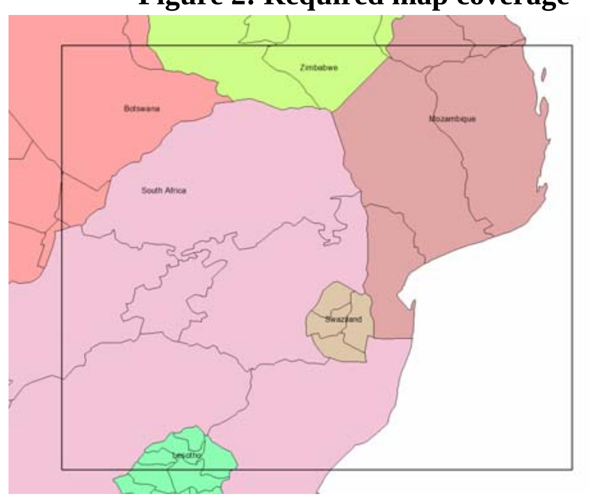

The map coverage will be within the bounding coordinates 21°S / 26°E to 29.5°S / 35.6°E (see Figure 2 below) and, providing approval is given by the end of September 2007, will be produced and hand carried to the Agency HQ in Vienna

These maps of modelled distributions are produced using multivariate analysis which is used to prepare 1km resolution predictions of fly distribution as used in previous studies[1]. These maps are of the probability of presence, which allows a significantly more refined assessment of risk than the simple presence or absence estimates used to define the models. They may also highlight areas which the original maps did not identify as suitable for the fly, and as well as those which were defined as suitable but are not. Details are provided in the Appendices

These models require considerable data acquisition and processing. The training data needed to calibrate the models are derived from the most accurate maps available, modified by factors such as

[1] Wint 2003 Kilometre resolution tsetse fly distribution maps for Southern Africa. Consultancy report and data CD for the Insect Pest Control Group, Food and Agriculture Organisation of the United Nations/IAEA Joint Division, International Atomic Energy Agency, Vienna, Austria.

high altitude and dense population or cultivation, that are known to limit the fly's range (see section on Masking variables). The climatic predictor data are derived from a substantial time series of several hundred satellite images processed to provide indicators seasonality and timing as well as the standard measures of temperature, and vegetation index. Full details are provided in the Appendices.

The deliverables for this work are thus defined as follows:

1) Establish and digitise both current and historical fly distributions. The historical extents describing the distribution of the components of the G. *morsitans* group are readily available from IAEA and collaborators but will require a modicum of processing.
2) Establish and digitise the precise boundaries of the new park and the connecting wildlife movement corridors.
3) Acquire and compile an agro-environmental predictor variable archive; compile distributions of current human population and cultivation intensity which are likely to restrict fly presence.
4) process time series satellite image predictor data archive to use in the distribution models. The most appropriate available imagery in the MODIS series which is available from 2001-2005, and has replaced the AVHRR imagery used in earlier Agency-commissioned vector mapping
5) Build distribution models and derive risk maps for current and historical distributions of G. *morsitans* and *G. pallidipes* within coordinates shown Figure 2.
6) Reporting and production of 10 laminated A2 maps.
7) Delivery of outputs to Vienna

2) Masking Variables

Figure 3: Masking Variables

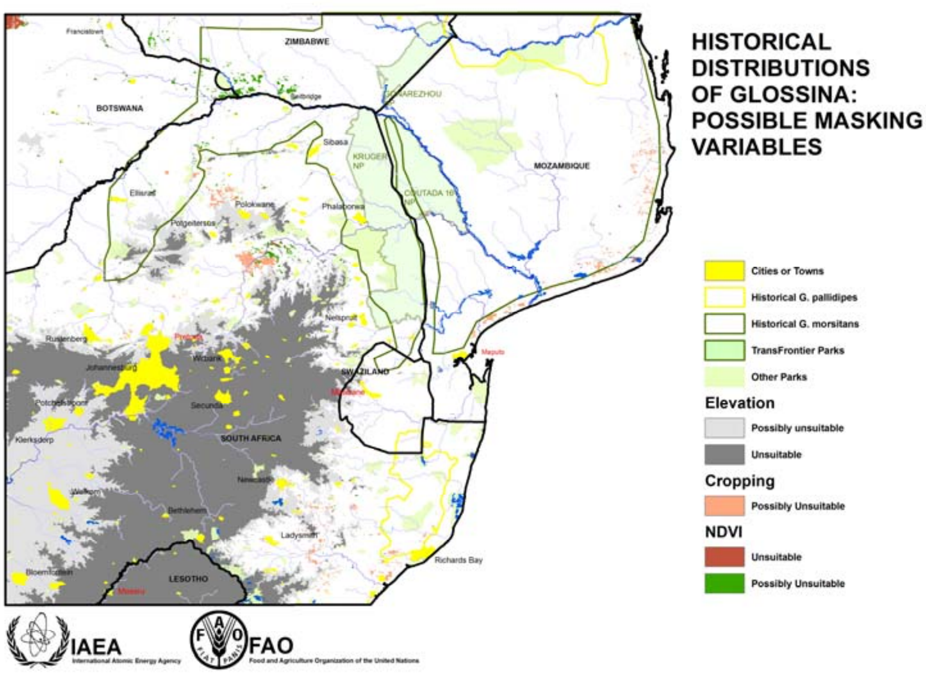

Whilst the models can be produced simply using the known or assumed distributions of the target vector species, they can be improved further by modifying both the input training data and the output model distributions with mask describing conditions that are unsuitable for the vectors. These include high altitudes and arid or hyper-arid conditions. Figure 3 maps the suitability limits for these two variables, and shows that none of the potential distribution for *G. palpalis*, and little of that for *G. morsitans* is overlapped by either parameter.

High cultivation levels tend to reduce the presence of tsetse flies, and so the known distributions of intense cropping can be also used to mask both the basic training distribution maps of the flies and the model outputs. A number of public domain sources of cultivation distributions are currently available, the most recent of which are the 1kilomter resolution Global Land Cover 2000 (GLC2K) dataset and a beta version of the 300m resolution GLOBCOVER (GC) product produced by the European Space Agency and collaborators at the Joint Research Centre in Ispra, Italy. Both include cultivation and cropping in their legends.

Before adopting these sources of information they were visually compared against Google Earth (GE) for central Mozambique and South-eastern Botswana. Figure 16 in Appendix 3 shows the GE coverage for the TFP. Figure 17 shows close-ups of an area within the brown circle in Figure 16, with both the GLC2K and GC distributions of cultivated land overlain. Not only do the coverages differ significantly, but both identify substantial cropping where GE shows none. Similar results were found in Southern Botswana (Figure 18), which suggests that these distributions are sufficiently flawed, at least for this part of southern Africa to preclude their use as accurate indicators of cultivation.

It was consequently decided to generate a cultivation map using the multivariate regression distribution modelling techniques employed to map the tsetse fly distributions, as described in Appendix 1, using the most recent available official administrative level survey and census data[2]. The results are shown in Figure 4, below, and can be compared with the values for administrative areas extracted. It can be seen that the fit between observed and predicted distributions is generally good – as also indicated by correlation coefficient of 0.818, (N=3223, Rsquared=0.67).

Figure 4: Modelled Cultivation level

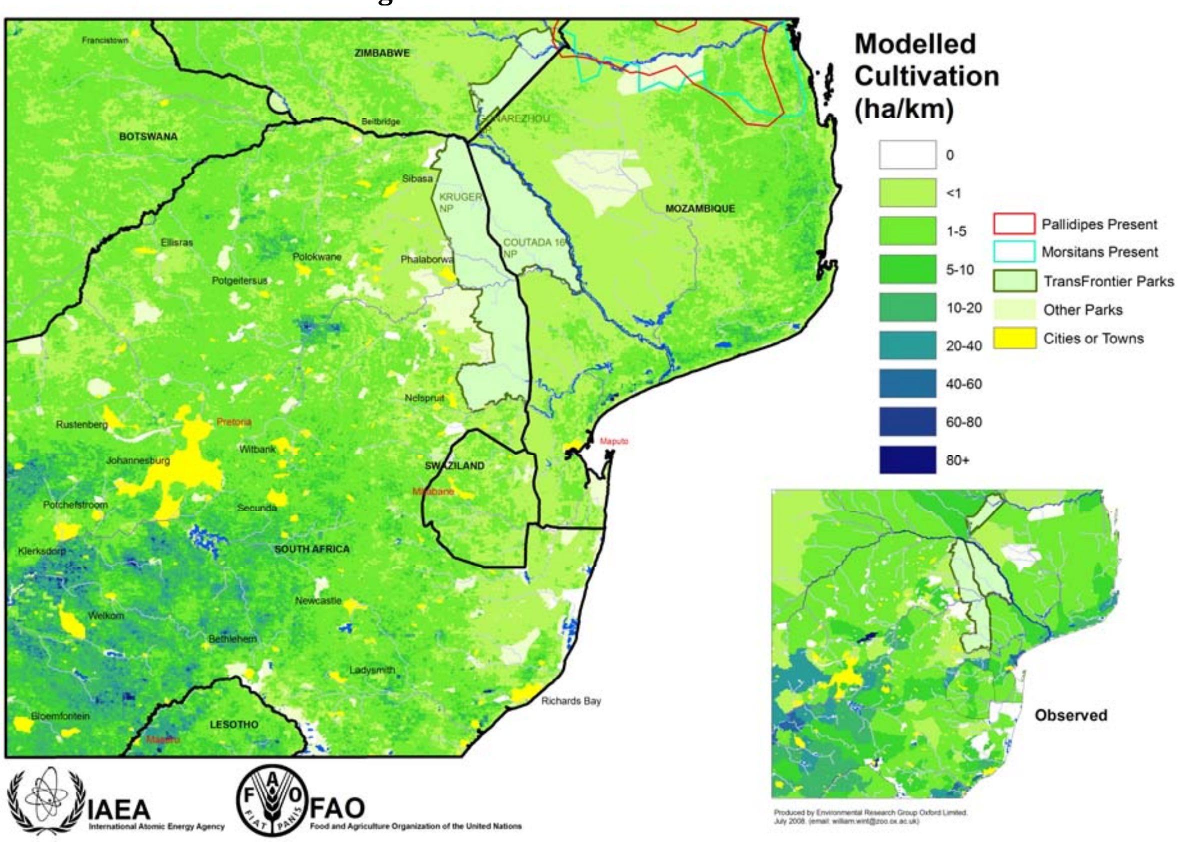

[2] Botswana Agricultural Census 2004; PAAT Information System, FAO 2000; South Africa Census of Agriculture 2002, Statistics south Africa; 2002 Crop and Food Supply Assessment Missions for Lesotho, Swaziland and Mozambique

3) Current Distributions of *G. morsitans* and *G. pallidipes*

Figure 5: 2003 model coverage

One of the deliverable items required is the mapped modelled distribution of the two tsetse fly species. That of *G. morsitans* was produced for IAEA covering Botswana, Zambia, Zimabwe and northern Mozambique in 2003 (for the area shown in Figure 5). Modelling of *G. pallidipes* distributions was not undertaken, though the input data were assembled and standardised.

Two alternatives thus presented themselves to produce predicted current distributions for these vectors: either to use the existing models for *morsitans* and the corresponding input datasets for *pallidipes*, thus suing models based on training data for a very extensive area; or to produce completely new models using only those data within the current area of interest, within which the vectors are present only in the north eastern margins.

Based on the assumption that model calibration should be based on as much data as possible, and in view of the fact that no new vector distribution data are available to use to revise the 2003 models, it was decided to use the 2003 datasets and extent, and to extract the portions for the area defined for this present work. Figure 6 thus shows the 2003 prediction for *G. morsitans*. Figure 7 shows the newly modelled distribution of *G. pallidipes*, based on the input datasets compiled in 2003, and using methods described in the Appendix.

Figure 6: Modelled current distribution of *G. morsitans*

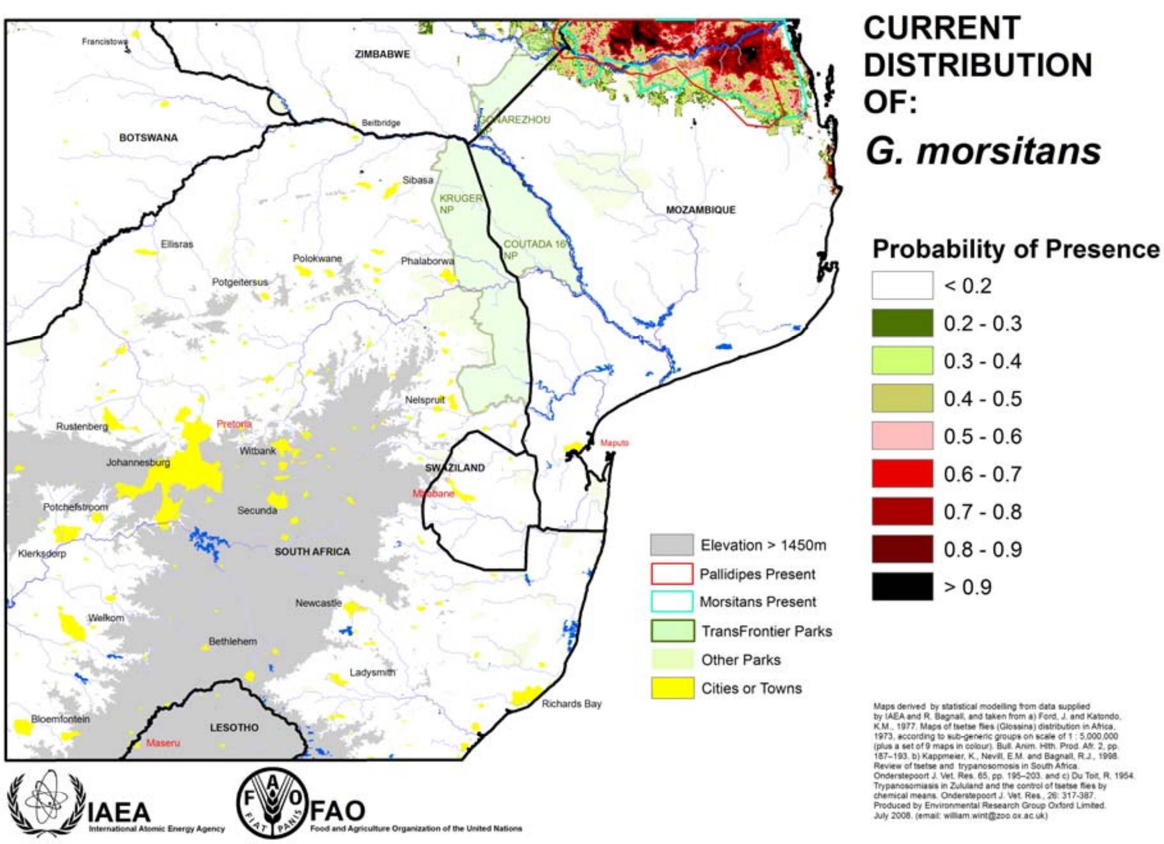

Figure 7: Modelled current distribution of *G. pallidipes*

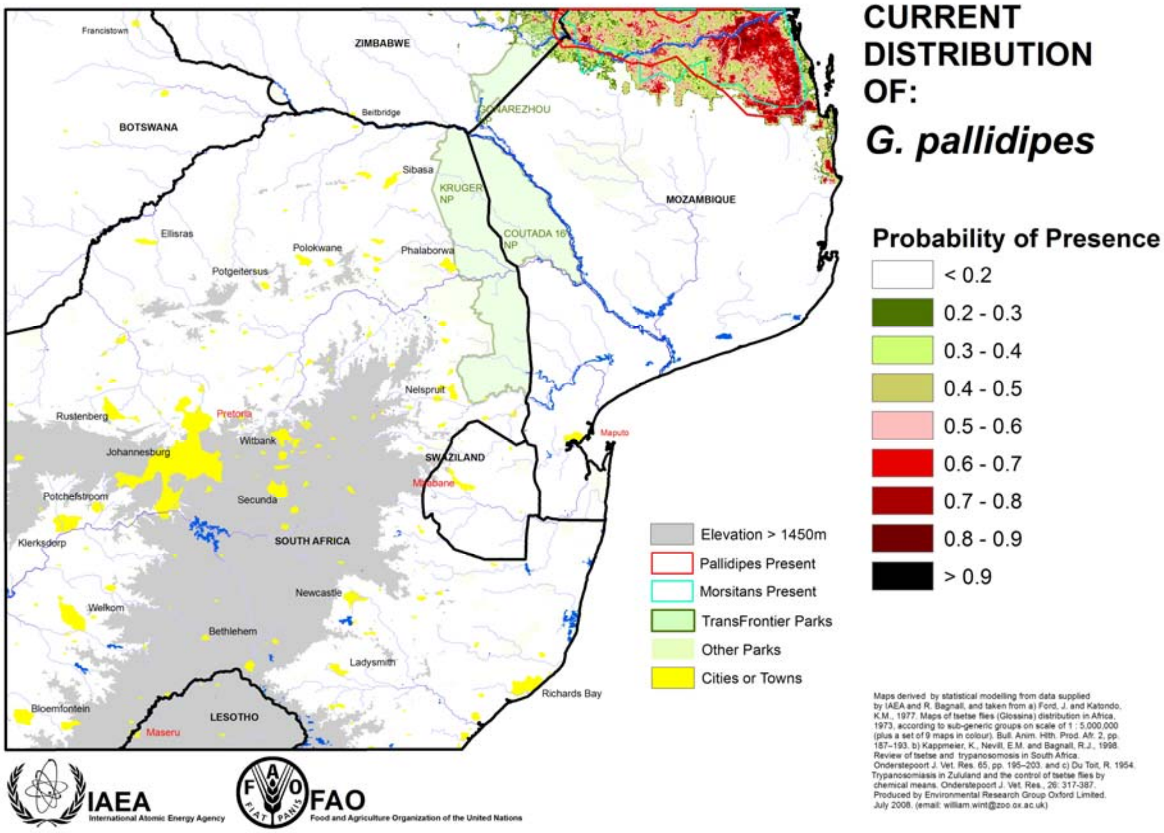

4) Historical distributions for *G. morsitans* and *G. pallidipes*

A range of graphic and textual sources have been made available to contribute to the definition of the likely historical limits of the two tsetse species:

Figure 8: Historical tsetse fly distribution: Kappmeier *et al*

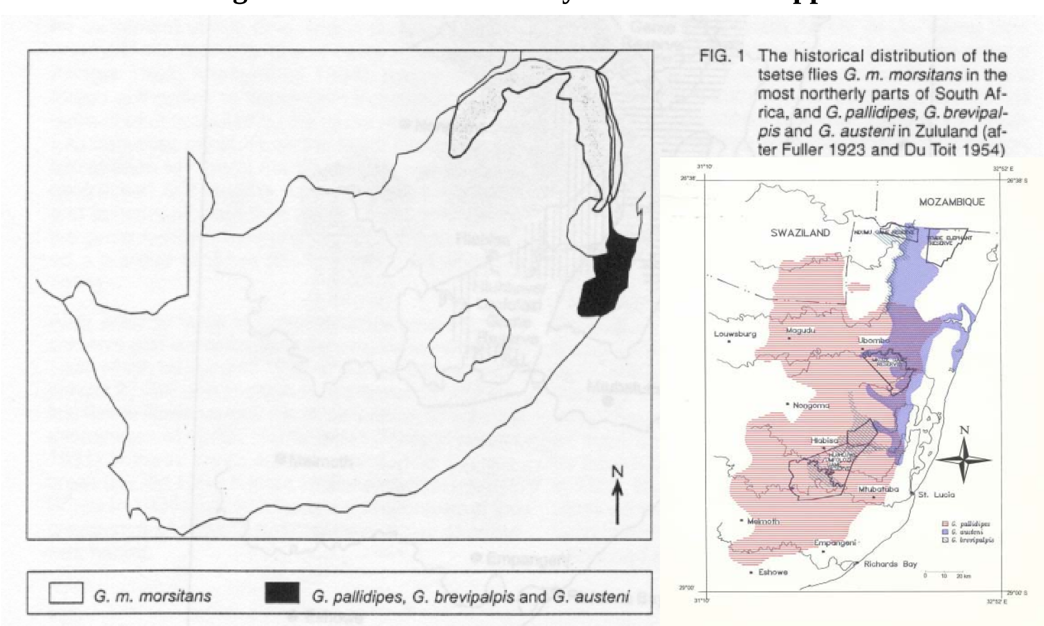

a) a paper by Kappmeier, Nevill and Bagnall[3], kindly provided by Rob Bagnall and supplemented by enhanced graphics of the Kappmeier figures from Marc Vreysen, IAEA. This details best available estimates of the southern historical distribution of *G. pallidipes* (Figure 8)

Figure 9: Historical tsetse fly distribution: du Toit

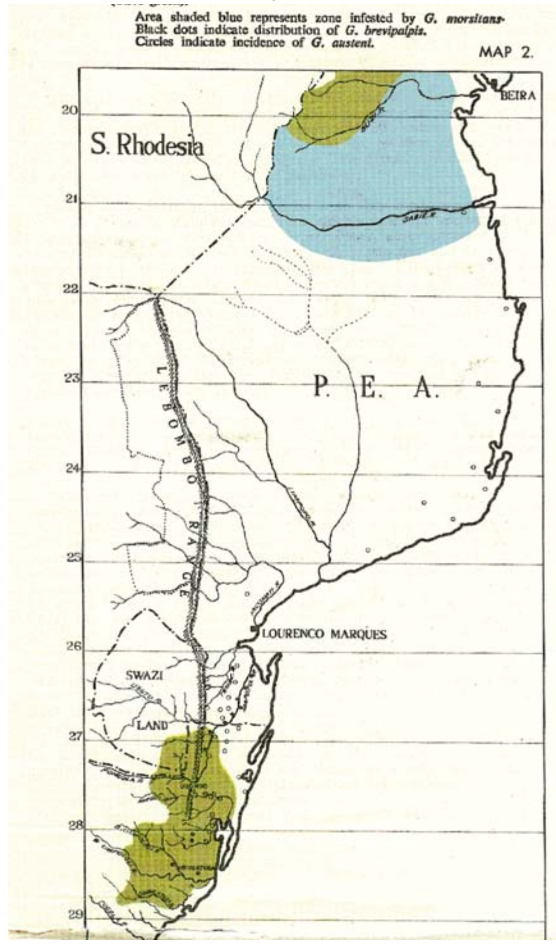

b) extracts from a paper by du Toit, 1954[4], which provides guidelines for the fly distributions in the mid fifties (Figure 9). In addition to the South African distribution of *G. pallidipes* repeated in Kappmeier *et al*'s publication, du Toit provides ranges for both fly species in 'Portugese East Africa, but also states:

"Fuller (1923) in discussing the incidence of the tsetse fly, G. *morsitans,* in the Transvaal, comes to the conclusion that its southernmost dispersion did not extend beyond the Umbeluzi river (latitude. 26^0 south) in northern Swaziland (see Map2) East of the Lebombo mountain range, within Portuguese 1erritory, it may have occupied country slightly south of this point, but the Tembe river appears to have marked its southernmost limit here. To the south a break of some 60 miles occurred in which no tsetse flies could be demonstrated." This suggests that the historical limits of *G morsitans* reached much further than the blue region shown in du Toit's maps, as far south as the vicinity of what is now Maputo.

Figure 10: Historical tsetse fly distribution: Bengis

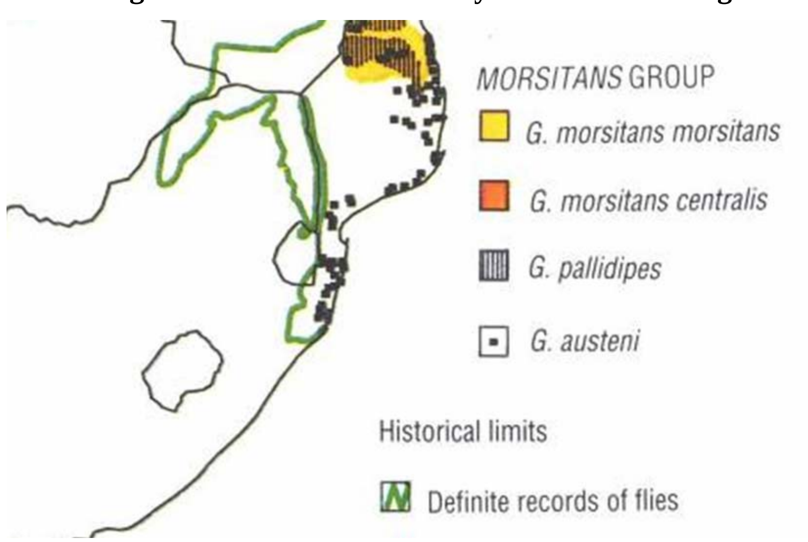

c) a series of powerpoint slides provided by Sarah Macfadyen at Kruger National Park, derived from a presentation produced by Roy Bengis (Figure 10). This concurs with both a) and b) in identifying current fly distributions in Mozambique, but historically two lobes of fly presence extending from southern Zimbabwe into north eastern South Africa (defined by Kappmeier *et al* as *morsitans)* with a further population south east of Swaziland (identified by du Toit and Kappmeier *et al* as *pallidipes).*

---

[3] Kappmeier, K., Nevill, E.M. and Bagnall, R.J., 1998. Review of tsetse and trypanosomosis in South Africa. Onderstepoort J. Vet. Res. 65, pp. 195–203.

[4] Du Toit, R. 1954. Trypanosomiasis in Zululand and the control of tsetse flies by chemical means. Onderstepoort J. Vet. Res., 26: 317-387.

Close examination also reveals that the definite historical distributions also extend from the south African border with Mozambique to the coast, though the flies are excluded from a narrow strip along the border itself, corresponding to the Lebombo Range. This agrees with Fullers reports of *morsitans* quoted in du Toit.

This evidence has been compiled into the single map shown below underlain by a map of altitude greater than 250m, with the minor modification that the Mozambique *morsitans* range has been removed from coastal areas – on the basis that this fly is not found near the coast in any other part of Africa (Figure 11).

Figure 11: Derived historical tsetse fly distribution

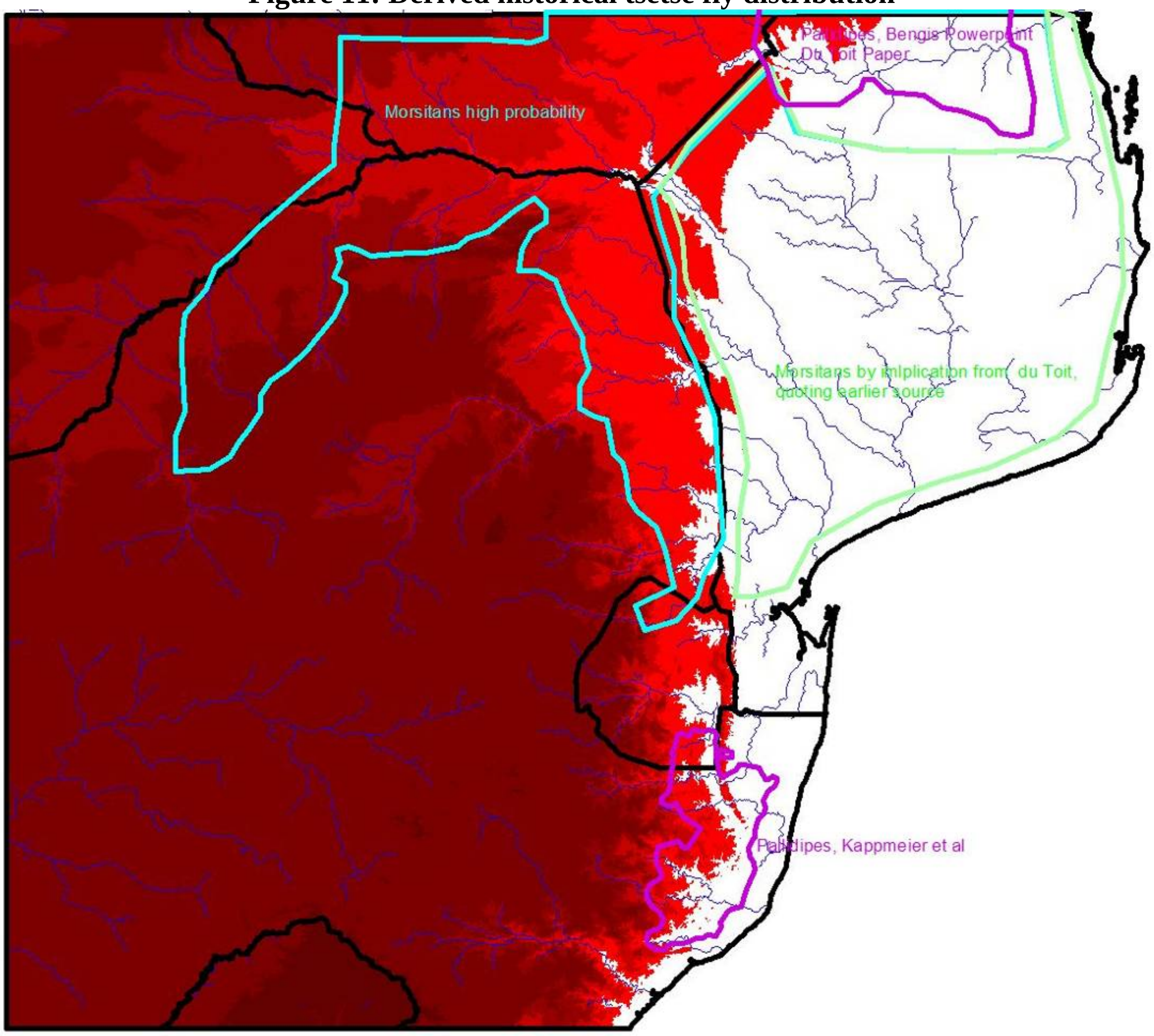

5) Modelled Historical Tsetse Fly Distributions

Distribution models were produced of each vector species, using the training distributions described in Section 4 above, and the methods set out in the Appendices. The outputs have also been masked so that tsetse distributions are set to absent in both the areas defined as unsuitable or possibly unsuitable. These areas are identified as those with elevation above 1250m, Normalised Difference Vegetation Index below 0.25, and cultivation above 10%. Despite the fact that these are very conservative values which would tend to exaggerate the area masked, very little of the predicted distributions are redefined as absent with these settings.

The modelled outputs for *G.morsitans* and *G. pallidipes* are shown on Figures 12 and 13 respectively. Both sets of predictions suggest that the historical distributions extended slightly beyond the training data bounds defined in Figure 11.

For *morsitans*, these areas include some regions to the west of Kruger National Parks, and in the south-eastern extremities of Botswana. The Lebombo mountain range, suggested by the earlier publications to be fly free is not predicted as being so, in line with the fact that their altitude is well below the limiting threshold usually set for tsetse fly distributions. It is, of course possible that there is some other environmental factor in these mountains that precludes tsetse presence, which, if identified, could be added to the masking criteria. Given the proximity of the two parallel lines in 11 that define this absence, it is, however, entirely possible that the absence is in fact an artefact of the graphics in the training data rather than a real absence.

For *pallidipes* the predicted historical distributions extend significantly to the south of the northern range, and northwards into Swaziland from southern range. There are also a number of patches throughout southern Mozambique where the fly is predicted to have been.

Figure 12: Modelled historical distribution: *G. morsitans*

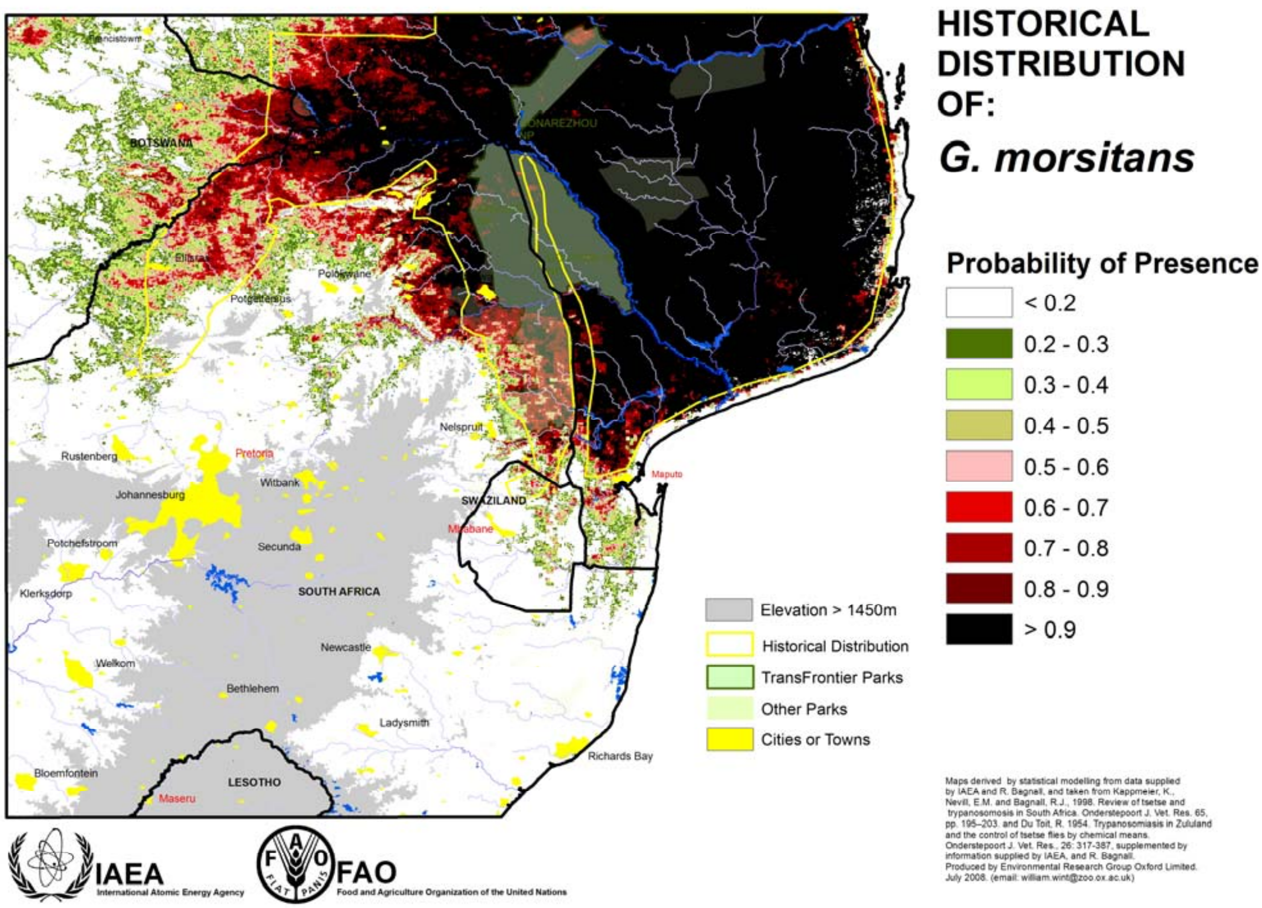

Figure 13: Modelled historical distribution: *G. pallidipes*

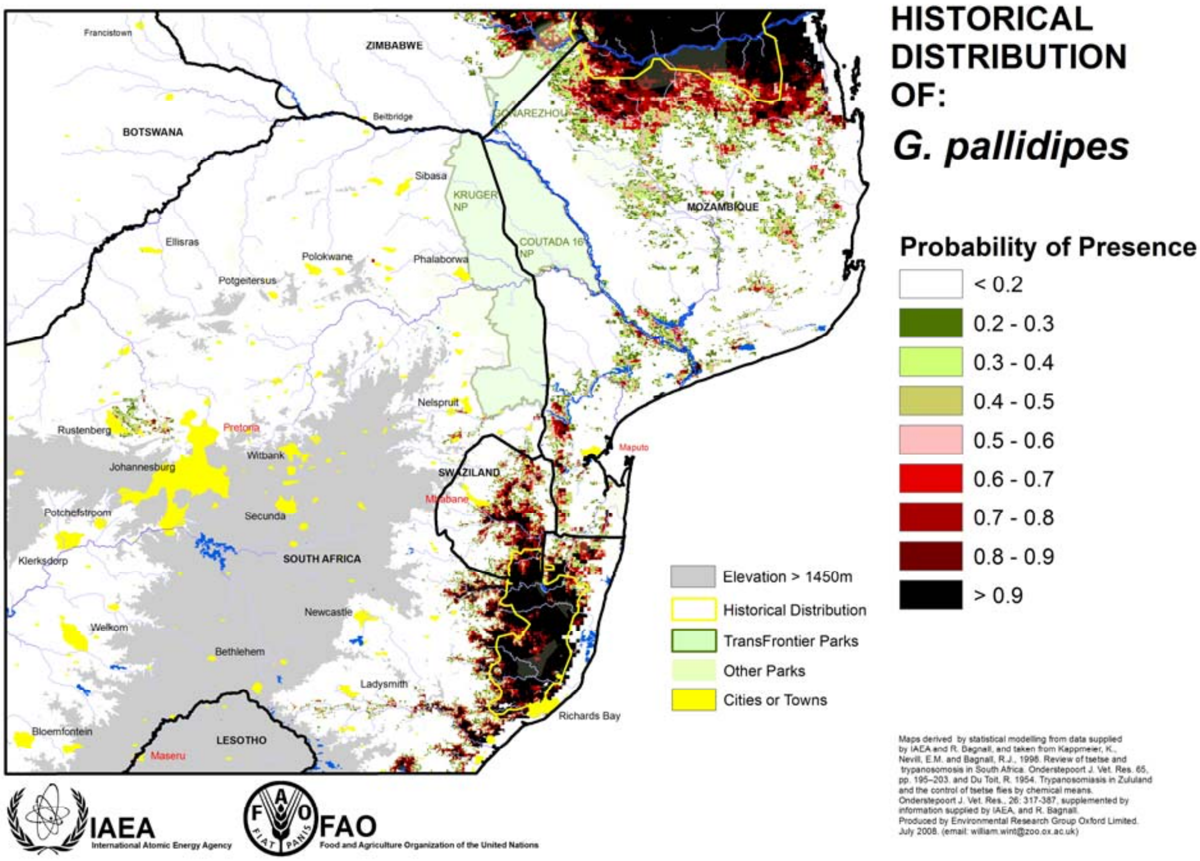

Appendix 1: Modelling

Statistical methods have been widely used for many years to produce maps of animal, plants and diseases, using largely environmental parameters as predictors of target variables, and so are particularly suited for use with insect vector data which are also likely to be linked to environmental criteria. These methods have been previously used to produce distribution models of a wide range of tsetse species throughout Africa.

The underlying processes of distribution modelling are summarised in Figure 14. Statistical relationships are identified between training data (*i.e.* known values of the parameters to be modelled) and the series of predictor variables, for a series of regularly spaced sample points approximately 50 kilometres apart. These relationships are then applied to a standardised series of rasterised predictor variable images to predict values at the resolution of the predictor images – in this case 1 kilometre. This results in a modelled distribution for areas between sample point locations.

Figure 14: Basic modelling procedure

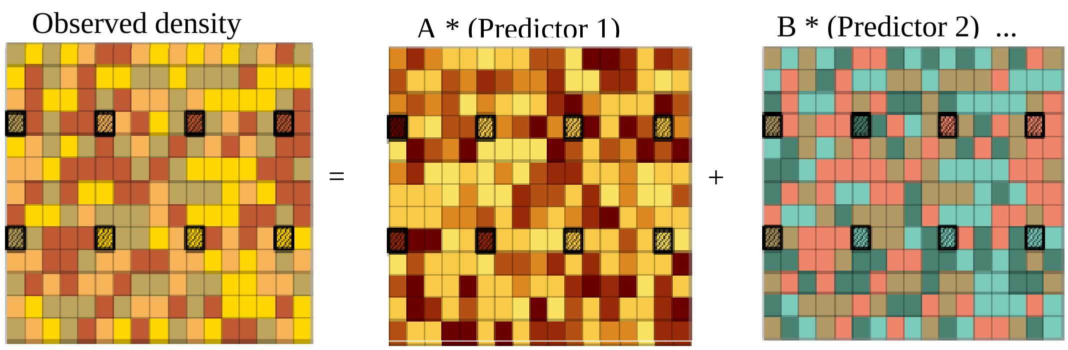

Step 1: Convert all data maps to images with same pixel size (resolution);
Step 2: Extract values for observations to be modelled at each tract, and for each predictor variable at the same sample points (hatched squares);
Step 3: Calculate a regression equation of the form:
Observed variable = Constant + A * (Predictor 1) + B * (Predictor 2) + ...;

Step 4: Providing the equation is statistically significant (*i.e.* reliable), apply the right hand side of the equation to **all** pixels in the predictor variable images to produce the predicted variable;
Step 5: Repeat the process for each of a series of analysis zones (e.g. ecozones).

Appendix 2: Predictor Archive

The statistical modelling technique relies on access to a wide range of predictor variables that can be used to define the relationships between target and predictor values. Because they are reliable surrogates for a wide range of environmental, ecological and climatic variables, satellite data are used to form the core of the distribution modelling predictor archive. These are also useful predictors because they are readily processed to derive summary climate and vegetation indicators with measures of seasonality and variability. Other indicators are, however, also likely to be useful as predictors, for example: demographic, topographic, hydrological, agricultural and infrastructural variables.

Following the compilation of appropriate training data and the selection and compilation of the predictor archive, the next important step in the modelling process is to compile a standardised predictor data file with values extracted for each analysis location. The final form of the extracted archive is thus a 'flat file' consisting of: 'point id, point x, point y, target variable 1, target variable 2, ... target variable *y*, predictor 1, predictor 2, predictor 3, … predictor *x*', which means that the input data may be point attribute values for the sample locations, polygon values extracted for each sample point using a spatial join tool (that assign data by location), or values extracted for each point from raster imagery. The image archive should ideally be a standard resolution and projection to simplify the extraction procedure, or at the very least collected into groups with a common resolution and projection. The image archive can be derived from other raster images, or, in the case of polygon data, converted from vector polygon to raster imagery.

About 80 parameters have been selected as predictors; the majority derived from extensive time series of remotely sensed climate or vegetation indicators. A number of sources were used: Moderate Resolution Imaging Spectroradiometer (MODIS) which replaces the Advanced Very High Resolution Radiometer (AVHRR) used in earlier work, and SPOT imagery from Europe. These include Day and Night-time Land Surface Temperature, Middle Infra Red, Normalised Difference Vegetation Index, Enhanced Vegetation Index, Potential Evapotranspiration and Precipitation.

Figure 15: MODIS processing

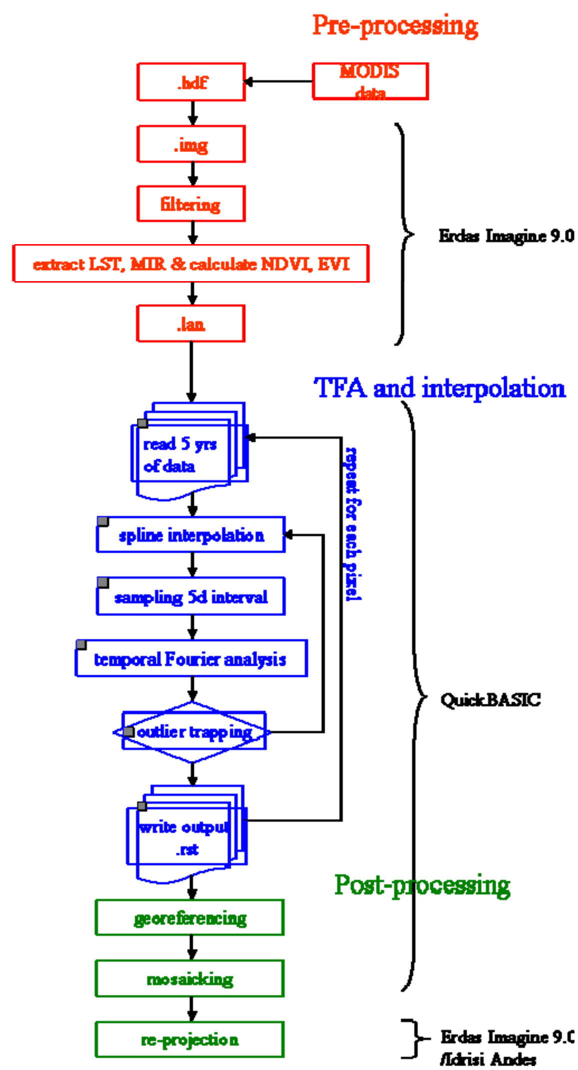

The MODIS imagery was downloaded from NASA, and processed according to the schema depicted in Figure 15. This was part of a collaborative undertaking with other projects led by the Spatial Epidemiology and Ecology Group at Oxford University's Department of Zoology, which has significantly improved both the quality and diversity of the output imagery. The quality control and data validation procedures have been enhanced by using a much wider geographical area to determine appropriate data quality thresholds, and test the robustness of image processing methods.

All are initially supplied as a series of monthly or decadal (10 day) images spanning several years, which amounts to several hundred images per variable – too many to include sensibly as predictor variables. As a result these data sets have been subject to temporal Fourier analysis, which produces a reduced set of biologically relevant variables for each parameter including the mean, two seasonality descriptors (phase and amplitude) for the first three Fourier components, as well as minima, maxima, range, and three estimates of variability. The Fourier process is also described in some detail Scharlemann *et al.* (2008)[5] for the MODIS imagery.

Additional variables, taken directly or derived from public domain global datasets, include: length of growing period, cultivation percentage; human population; elevation; slope; and proximity to roads, rivers and built up areas derived using standard GIS procedures.

[5] Scharlemann, J.P.W, Benz, D., Hay, S.I., Purse, B.V., Tatem, A.J., Wint, G.R.W. and Rogers, D.J. (2008) Global data for ecology and epidemiology: A novel algorithm for temporal Fourier processing of MODIS data. *PLoS ONE* 3(1): e1408. doi:10.1371/journal.pone.0001408.

Table 1 details the predictor archive properties – filenames, sources, data type and units and processing type and personnel. These are all provided in ArcGIS 9.2 compatible format raster images (either Idrisi 32 or ESRI Grid) The images are at 1km resolution and are all contained in a Winzip archive: *iaeasatfpimg.zip*.

Table 1: Predictors and Stratification Criteria

Predictor Variable	Filename	Units	Source	Processing
Evapotranspiration	step*	Scaled,	VGT4AFRICA, Vito Belgium	Fourier, by SEEG and ERGO[1]
Precipitation	stpp*	mm	VGT4AFRICA, Vito Belgium	Fourier, by SEEG and ERGO[1]
Normalised difference vegetation Index	Sg15*	Scaled index	MODIS, NASA	Fourier, by SEEG and ERGO[1]
Enhanced vegetation index	sg14*	Scaled index	MODIS, NASA	Fourier, by SEEG and ERGO[1]
Night Land Surface Temperature	Sg08*	Scaled Temperature	MODIS, NASA	Fourier, by SEEG and ERGO[1]
Day Land Surface Temperature	Sg07*	Scaled Temperature	MODIS, NASA	Fourier, by SEEG and ERGO[1]
Middle Infra Red	Sg03*	Scaled Temperature	MODIS, NASA	Fourier, by SEEG and ERGO[1]
Length of Growing Period	stlgpr	Days	MODIS, NASA	Modelled, by ERGO
Human Population density	stgpw3dn	Density/sq km	Global Population of the World, CEISIN	None
Elevation	ststrm1k	Meters	Shuttle Radar Topography Mission, NASA	None
Slope	Stslpll	index	Shuttle Radar Topography Mission, NASA	Derived by ERGO
Distance to Roads	strdsdg	degrees	Derived from Roads layer in Landscan Dataset	Derived by ERGO
Distance to Nighttime lights	stlgtdg	degrees	Derived from Nighttime lights layer in Landscan Dataset	Derived by ERGO
Distance to Rivers	stfprvdg	degrees	Derived from USGS Hydro1k datasets	Derived by ERGO
Small water bodies 2001	stswbp1	Proportion of year with water	VGT4AFRICA, Vito Belgium	Derived by ERGO
Small water bodies 2002	stswbp2	Proportion of year with water	VGT4AFRICA, Vito Belgium	Derived by ERGO
Small water bodies 2003	stswbp3	Proportion of year with water	VGT4AFRICA, Vito Belgium	Derived by ERGO
Small water bodies 2004	stswbp4	Proportion of year with water	VGT4AFRICA, Vito Belgium	Derived by ERGO

[1]: See Tables 2 for Fourier Variable scaling and Table 3 for Fourier Variable naming conventions Processing details of remotely sensed imagery provided above.

Table 2: MODIS Image Values, Rescaling Criteria

Parameter	Fourier Variable	Image values are
MIR (03)	A0, A1, A2, A3, Min, Max, Var	Reflectance values * 10000
LST (07,08)	A0, A1, A2, A3, Min, Max, Var	(Degrees Centigrade+273)*50
NDVI (14) and EVI (15)	A0, A1, A2, A3, Min, Max,	(Index Value * 1000) -1
ET	A0, A1, A2, A3, Min, Max,	Mm/10days
NDVI (14) and EVI (15)	VAR	Value * 10000
ALL	D1,D2,D3,Da	Percentages
ALL	E1,E2,E3	Percentages
ALL	P1,P2.P3	Months*100. (Jan=1)

Table 3:MODIS image files, Naming conventions.

A) Fourier Processed Files: ABCDEEPP.EXT.

A Location	B Projection	C Start Year	D End Year	EE Climate Parameter	FF Fourier Variable and Component	EXT File Type
S= Southern Africa	G=Geographic S=MODIS Sinusoidal	0=2000	5=2005	03=MIR	A0=Mean	RST, RDC = Idrisi raster and document files
		1=2001		07=dLST	A1,2,3=Amplitude	IMG=ERDAS Imagine raster
				08=nLST	P1,2,3=Phase	
				14=NDVI	D1,2,3=Proportion total variance from each Component. DA=All	
				15=EVI	MN, MX, RN=Min, Max, Range	

Appendix 3: Land Cover Layer Validation

A comparison of Cultivation categories in Land Cover maps with Google Earth suggests that the areas defined as cultivated by either the Global Land Cover 2000 or the draft GLOBCover Land cover/Land use datasets (Figure 16) are shown as cultivated by the aerial photography coverage provided by Google Earth (Figure 17) A similar result is shown for the area where the borders of Zimbabwe, Bostwana and South Africa meet (Figure 18)

Figure 16: Land Cover Validation: Google Earth Coverage of Area highlighted in inset left

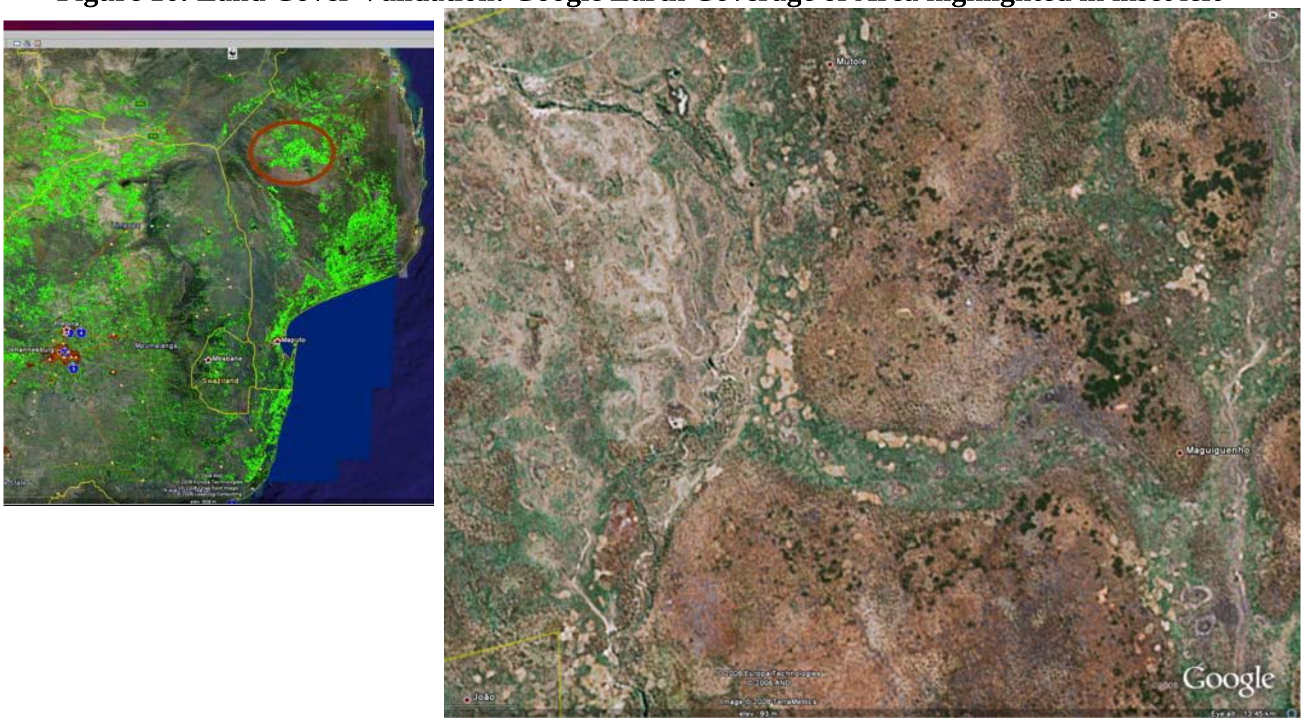

Figure 17: Land Cover Validation: Cultivation in Land Use/Cover Datasets

Global Land Cover 2000, JRC, Ispra Draft GlobCover 2008, ESA, Jrc

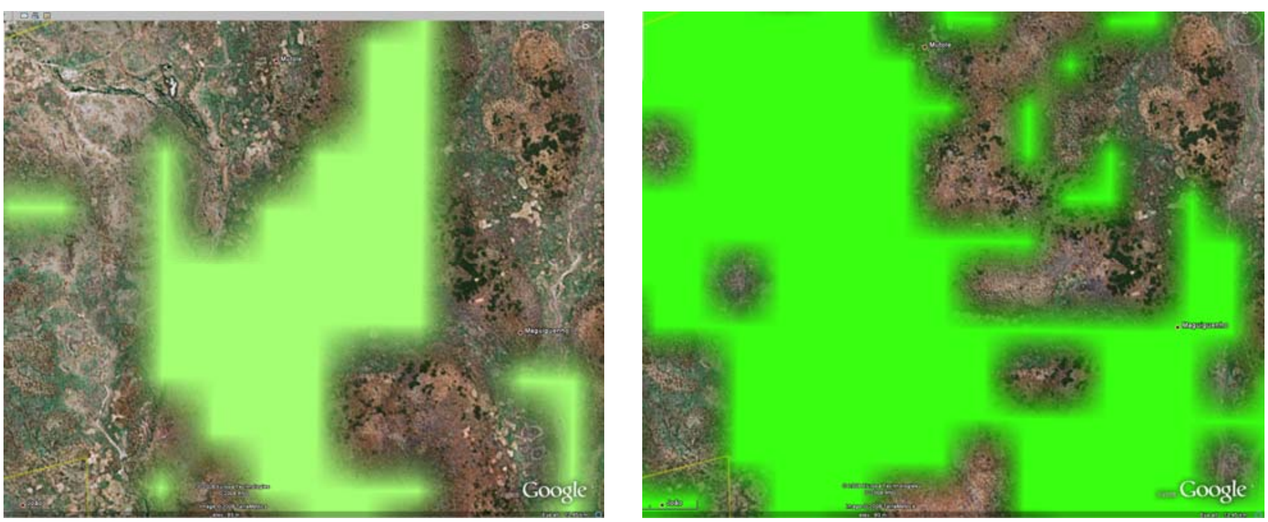

Figure 18: Land Cover Validation: Global Land Cover 2000, Zimbabwe/Botswana/South Africa border

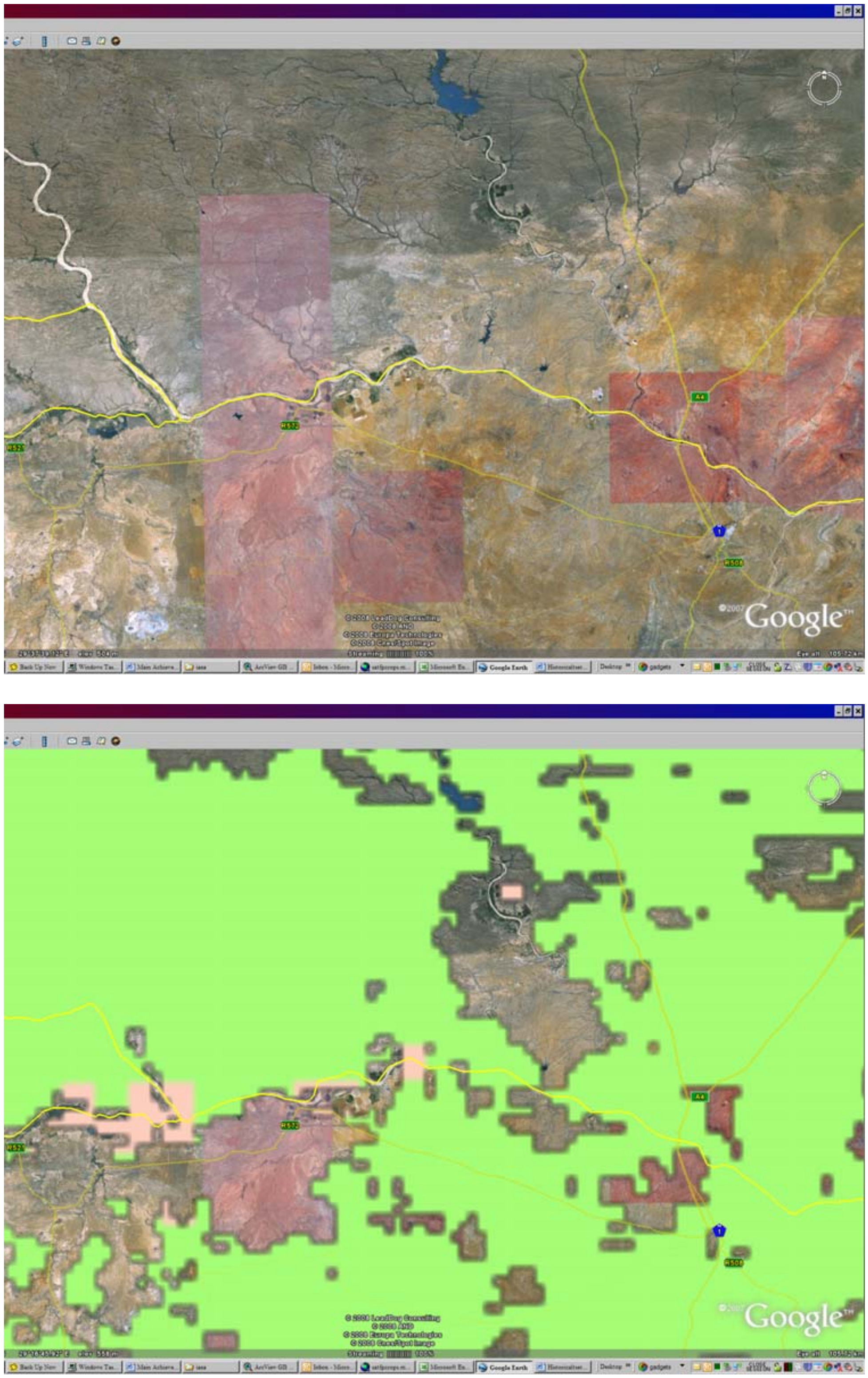

Appendix 4: Datasets supplied

All spatial data is supplied in EDSRI ArcGIS 9.2 compatible format. Document (mxd) files are also supplied, which will require opening and assume the data are stored in the same folder structure as supplied. If the folder structure is changed then the data sources will require 'repairing' within each document file.

The maps are also supplied in Adobe pdf format and in reduced resolution .jpg image format for use in presentations or documents.

All maps and images are A2 size.

Table 4: Data files supplied.

Folder	Filename	File Type	File Content
\iaeasatfp	Historicaltsetse.doc	Word Document	This report
	Historicaltsetse.pdf	Adobe pdf	This report
	satfpark.shp	Shape	Transfrontier Parks
	satfpother.shp	Shape	Other Parks
	stfplgt	Grid Folder	City Lights
	stfpwat1km	Grid Folder	Water Bodies
	stfprvll.shp	Shape	Rivers
	histpallidipes.shp	Shape	Historical G. pallidipes
	histmorslimits.shp	Shape	Historical G. morsitans
	satfpmask0	Grid Folder	Country/Land Mask
	saftpcountry.shp	Shape	Country Boundaries
	tsepres.shp	Shape	Current Tsetse Presence
	Satfpmapfiles.xls	Excel sheet	This table
\iaeasatfp	Historicaltsetse.doc	Word Document	This report
\iaeasatfp\prestse	morspred	Grid Folder	Predicted Current morsitans presence
	pallidpred	Grid Folder	Predicted Current pallidipes presence
\iaeasatfp\predimg	ststrm1k.rst	Idrisi Raster	Elevation
	stcpcprc.rst	Idrisi Raster	Predicted Cropping percentage
	STHPAL10PR5.RST	Idrisi Raster	Predicted Historical pallidipes presence
	STHMORPR.RST	Idrisi Raster	Predicted Historical morsitans presence
	stpccpc.rst	Idrisi Raster	Observed cropping percentage
\iaeasatfp\maps	satfphistpallpreda2.mxd	ArcMap Document	Historical pallidipes presence map
	satfphistpallpreda2.pdf	Adobe pdf	Historical pallidipes presence map
	satfphistpallpreda2.jpg	JPG image	Historical pallidipes presence map
	satfphistmorspredA2.mxd	ArcMap Document	Historical morsitans presence map
	satfphistmorspredA2.pdf	Adobe pdf	Historical morsitans presence map
	satfphistmorspredA2.jpg	JPG image	Historical morsitans presence map
	satfppallcurrentpredA2.mxd	ArcMap Document	Current pallidipes presence map
	satfppallcurrentpredA2.pdf	Adobe pdf	Current pallidipes presence map
	satfppallcurrentpredA2.jpg	JPG image	Current pallidipes presence map
	satfpmorscurrentpredA2.mxd	ArcMap Document	Current morsitans presence map
	satfpmorscurrentpredA2.pdf	Adobe pdf	Current morsitans presence map
	satfpmorscurrentpredA2.jpg	JPG image	Current morsitans presence map
	satfpcropsA2.mxd	ArcMap Document	Predicted Cropping percentage
	satfpcropsA2.pdf	Adobe pdf	Predicted Cropping percentage
	satfpcropsA2.jpg	JPG image	Predicted Cropping percentage
	Satfpdemenvmaska2.mxd	ArcMap Document	Possible masking variables